Clim Dyn
DOI 10.1007/s00382-014-2069-9

Thirty-two-year ocean–atmosphere coupled downscaling of global reanalysis over the Intra-American Seas

Haiqin Li · Vasubandhu Misra

Received: 27 September 2013 / Accepted: 22 January 2014

Abstract This study examines the oceanic and atmospheric variability over the Intra-American Seas (IAS) from a 32-year integration of a 15-km coupled regional climate model consisting of the Regional Spectral Model (RSM) for the atmosphere and the Regional Ocean Modeling System (ROMS) for the ocean. It is forced at the lateral boundaries by National Centers for Environmental Prediction-Department of Energy (NCEP-DOE R-2) atmospheric global reanalysis and Simplified Ocean Data Assimilation global oceanic reanalysis. This coupled downscaling integration is a free run without any heat flux correction and is referred as the Regional Ocean–Atmosphere coupled downscaling of global Reanalysis over the Intra-American Seas (ROARS). The paper examines the fidelity of ROARS with respect to independent observations that are both satellite based and in situ. In order to provide a perspective on the fidelity of the ROARS simulation, we also compare it with the Climate Forecast System Reanalysis (CFSR), a modern global ocean–atmosphere reanalysis product. Our analysis reveals that ROARS exhibits reasonable climatology and interannual variability over the IAS region, with climatological SST errors less than 1 °C except along the coastlines. The anomaly correlation of the monthly SST and precipitation anomalies in ROARS are well over 0.5 over the Gulf of Mexico, Caribbean Sea, Western Atlantic and Eastern Pacific Oceans. A highlight of the ROARS simulation is its resolution of the loop current and the episodic eddy events off of it. This is rather poorly simulated in the CFSR. This is also reflected in the simulated, albeit, higher variance of the sea surface height in ROARS and the lack of any variability in the sea surface height of the CFSR over the IAS. However the anomaly correlations of the monthly heat content anomalies of ROARS are comparatively lower, especially over the Gulf of Mexico and the Caribbean Sea. This is a result of ROARS exhibiting a bias of underestimation (overestimation) of high (low) clouds. ROARS like CFSR is also able to capture the Caribbean Low Level Jet and its seasonal variability reasonably well.

Keywords Coupled downscaling · Reanalysis · Intra-American Seas · Interannual variability

H. Li (✉) · V. Misra
Center for Ocean-Atmospheric Prediction Studies, Florida State University, Tallahassee, FL, USA
e-mail: haiqin.li@fsu.edu

V. Misra
Department of Earth, Ocean and Atmospheric Science, Florida State University, Tallahassee, FL, USA

V. Misra
Florida Climate Institute, Florida State University, Tallahassee, FL, USA

1 Introduction

The Intra-American Seas (IAS), which broadly covers the regions of Caribbean Sea, Gulf of Mexico, and parts of north western Atlantic Ocean is a vital source of moisture over the continental US both in the summer (Ruiz-Barradas and Nigam 2005; Mo et al. 2005) and winter (Orlanski and Sheldon 1995; Bosart and Lin 1984). Yet intriguingly IAS is one of the poorly observed parts of the global oceans (Misra et al. 2009). The IAS circulation system is a complicated western boundary current system. The Caribbean Current transports significant amounts of warm water that flows northwestward through the Caribbean Sea from the east along the coast of South America and into the Gulf of Mexico. When the

Published online: 02 February 2014

current turns north through the Yucatan Channel, it becomes known as the Yucatan Current. Then it becomes the Loop Current as it flows northward between Cuba and the Yucatan Peninsula, which moves north into the eastern Gulf of Mexico. The Loop Current then turns anticyclonically southward to exit to the east through the Florida Straits and joining the Gulf Stream (Mooers and Maul 1998). One of the best-known mesoscale variability in the IAS is an area of warm water with an "eddy" or "Loop Current ring" that separates from the Loop Current, somewhat randomly every 3–17 months (Oey et al. 2005). These eddies are critical to redistribute heat to the western part of the Gulf of Mexico (Chang and Oey 2010; Liu et al. 2012).

Recent numerical ocean modeling studies have proved that high resolution is necessary to resolve the oceanic features over the IAS. The first successful numerical simulation of loop current and eddies off it follows from Hurlburt and Thompson (1980), which was at 20 km grid resolution. Subsequent studies have clearly shown the benefit of high-resolution ocean models in resolving these oceanic features in the IAS region (Chérubin et al. 2005, 2006). Chassignet et al. 2005 showed that the horizontal resolution is important to represent the Loop Current and associated rings, e.g., Navy Costal Ocean Model (NCOM) 1/8° system doesn't perform as well as NRL Layered Ocean Model (NLOM) 1/16° and Hybrid Coordinate Ocean Model (HYCOM) 1/12° systems. In another related study, Oey et al. 2005 also demonstrated that a 20 km or even higher resolution is needed to properly resolve the strength, position and eddy shedding characteristics of the Loop Current. A downscaled high-resolution ocean model with a horizontal resolution of 0.1° over Gulf Mexico successfully predicted the reduced Loop Current in twenty-first century, while the low resolution models underestimate the reduction of Loop Current and its cooling effect (Liu et al. 2012).

The IAS is a source of moisture and energy to a number of severe weather events spread across the year over continental North America including seasonal and long-term flooding and drought events over the mid-western United States (Rasmusson 1967; Bosilovich and Schubert 2002; Ruiz-Barradas and Nigam 2005; Wang et al. 2006; Mestas-Nuñez et al. 2007; Chan and Misra 2010). The IAS is not only a host to complex fine scale intricate ocean surface currents (Sturges and Lugo-Fernandez 2005), but also is host to many fine scale atmospheric features such as the Caribbean Low Level Jet (Amador 2008), and genesis region for many tropical cyclones and even winter storms (e.g. President's day storm; Bosart and Lin 1984; blizzard of 1993; Orlanski and Sheldon 1995). Therefore the importance of using ocean–atmosphere coupled models to understand ocean–atmosphere interactions of this region cannot be overemphasized.

Coupled ocean–land–atmosphere modeling, a subset of the earth system models has been promoted in the recent literature for seamless prediction of weather and climate (Palmer et al. 2008; Hurrel et al. 2009; Shukla et al. 2010). There is a growing consensus that coupling is critical for the simulation of monsoon variations and variability of the upper ocean in critical regions of the tropical and subtropical oceans (Wang et al. 2005; Wu et al. 2006; Misra 2008a). It is shown that air–sea interactions promote improved land–atmosphere coupling over the continental regions (Misra 2008a, b; Misra and Dirmeyer 2009). Similarly Wu et al. (2006) show that in many regions of the tropical and subtropical oceans the atmospheric fluxes dictate the SST variations. Misra et al. (2009) show that the wind induced evaporation plays a critical role in the regulation of the SST over the IAS.

A fully coupled regional ocean–atmosphere modeling system, which contains the Regional Spectral Model (RSM, Juang and Kanamitsu 1994; Kanamitsu et al. 2010) for the atmosphere and the Regional Ocean Modeling System (ROMS, Shchepetkin and McWilliams 2005), has been developed recently. This RSM–ROMS coupled modeling system has been previously used in the 10-km downscaling of global reanalysis over California Current System (Li et al. 2012) and regional climate change projection studies over California (Li et al. 2013a, b). The coupled downscaling shows much more realistic ocean and atmospheric states than the uncoupled downscaling, and the air–sea coupling plays an important role in the simulation of coastal mesoscale circulation. However, the heat flux correction was applied in the previous studies (Li et al. 2012, 2013a, b), and the oceanic variability in those simulations was not extensively investigated.

The purpose of this study is to establish the fidelity of RSM–ROMS in capturing the climatology and interannual variability of the IAS region when it is forced with global reanalysis before we embark on conducting any further studies with global predictions and projections. In this study we present the results from Regional Ocean–Atmosphere coupled downscaling of global Reanalysis over the Intra-American Seas (ROARS), which is a 32-year integration free run without any heat flux correction. A series of in situ and satellite observations will be used to validate ROARS. The latest state-of-the-art high resolution National Centers for Environmental Prediction (NCEP) Climate Forecast System Reanalysis (CFSR; Saha et al. 2010) is also used to validate ROARS. This comparison of ROARS with CFSR is done to provide a perspective on the fidelity of ROARS since CFSR provides both global atmospheric and oceanic reanalysis. CFSR is the closest that we have to a "coupled" global reanalysis of the atmosphere and the ocean. Therefore comparing ROARS with CFSR would shed some light on the prospect of using uncoupled global reanalysis of the atmosphere and the ocean to force a regional coupled ocean–atmosphere model

to produce a "pseudo" regional reanalysis for the IAS region. It should however be remembered ROARS is not ingesting any observations during its integration period, which is unlike CFSR that ingests a variety of observations throughout its assimilation period.

This paper is organized as follows. In Sect. 2, the regional coupled model and experiments are described. The description of observational datasets and CFSR used for validation is presented in Sect. 3. Section 4 discusses the results of the coupled downscaling over IAS forced by the global reanalysis of the atmosphere and the ocean with final concluding remarks in Sect. 5.

2 Description of model and experiments

2.1 The regional coupled model

A fully coupled regional ocean–atmosphere modeling system, which contains the Regional Spectral Model (RSM; Juang and Kanamitsu 1994; Juang et al. 1997; Kanamitsu et al. 2010) as the atmospheric part and the Regional Ocean Modeling System (ROMS; Haidvogel et al. 2000; Shchepetkin and McWilliams 2005) as the oceanic component, is utilized in this study. This RSM–ROMS coupled modeling system has been previously used in the downscaling of global reanalysis centered over California (Li et al. 2012) and regional climate change projection studies over California (Li et al. 2013a, b). A brief description of the regional ocean–atmosphere coupled model is presented here. The readers are referred to Li et al. (2012) for further details on the regional modeling system.

The RSM is a primitive equation atmospheric model. The RSM uses a spectral method (with sine and cosine series) in two dimensions (Juang and Kanamitsu 1994). The RSM has 28 terrain following sigma levels, with irregular spacing in the vertical that is identical to the NCEP-DOE reanalysis (R2; Kanamitsu et al. 2002), and the top of the atmosphere in RSM is at $\sim$2 hPa. The RSM physical schemes used in this study is listed in Table 1. The cloudiness is computed from relative humidity, vertical motion, and the depth of the marine boundary layer (Slingo 1987). These clouds interact with the short and longwave radiation schemes following (Chou and Suarez 1994; Chou and Lee 1996). The Scale Selective Bias Correction (SSBC, Kanamaru and Kanamitsu 2007, Kanamitsu et al. 2010) is used to prevent synoptic scale drift during the regional climate model integration. The ROMS is a free-surface, terrain-following, primitive equation ocean model. It was based on the S-coordinate Rutgers University Model (SCRUM, Song and Haidvogel 1994). The RSM and ROMS are coupled by using the efficient MPI dual coupling scheme with a coupling interval of 24-h.

Table 1 RSM physics

	Parameterization	References
Convection	Relaxed Arakawa-Schubert	Moorthi and Suarez (1992)
Shallow convection	Tiedtke scheme	Tiedtke (1983)
Boundary layer	Nonlocal scheme	Hong and Pan (1996)
Longwave radiation	M.-D. Chou	Chou and Suarez (1994)
Shortwave radiation	M.-D. Chou	Chou and Lee (1996)
Cloud	Slingo	Slingo (1987)
Gravity wave drag	Pierrehumbert	Alpert et al. (1988)
Land model	NOAH LSM	Ek et al. (2003)

The RSM and ROMS share the same domain and resolution to avoid interpolation between atmosphere and ocean model grids. The SST-flux is directly exchanged between RSM and ROMS without using any SST-flux coupler.

2.2 Experiments

The ROARS was conducted with this RSM–ROMS regional coupled model. The domain of ROARS is shown in Fig. 1. The domain (8.002°S–38.391°N, 100.49°W–44.097°W) covers Southeastern US, Central America, Northern part of South America, and the IAS. Four sub-domains of Gulf of Mexico (GM), Caribbean Sea (CS), Eastern Pacific (EP), and Western Atlantic (WA) as outlined in Fig. 1 are used to analyze the oceanic variability. The 15 km horizontal resolution is identical for both RSM and ROMS. The RSM has 28 vertical atmosphere sigma levels, while ROMS has 30 vertical ocean sigma levels. The atmospheric lateral forcing and initial conditions is taken from T62L28 R2 Reanalysis (Kanamitsu et al. 2002). The monthly Simple Ocean Data Assimilation (SODA, Carton et al. 2000) is used for the oceanic initial and boundary condition. SODA is available at 0.5° horizontal resolution with 40 vertical layers.

It may be noted that this coupled downscaling is a free run without any heat or salinity flux corrections. The thirty-two-year integration period is from 1979 to 2010. The first 2 years are discarded in the analysis to account for spin-up. The remaining 30 years of the ROARS integration are used for analysis of the results.

3 Datasets

3.1 In situ and satellite observations

This study utilizes a mix of in situ observations, satellite based datasets, and multi-sensor analysis for validation of

ROARS as listed in Table 2. We also compare ROARS with the relatively new Climate Forecast System Reanalysis (CFSR; Saha et al. 2010). CFSR is a coupled global ocean–atmosphere reanalysis that is current and makes use of a global coupled ocean–atmosphere model. The wind stress climatology is validated with the Quickscat Scatterometer Climatology of Ocean Winds (SCOW, Risien and Chelton 2008), which is available from September 1999 to October 2009. The 925 hPa wind speed from Integrated Global Radiosonde Archive (IGRA, http://www.ncdc.noaa.gov/oa/climate/igra/) over Plesman Field (68.97°W, 12.2°N) is used to validate the Caribbean Low-Level Jet. The monthly CPC Merged Analysis of Precipitation (CMAP, Xie and Arkin 1997) is used to validate the climatology and variability of precipitation. The pentad CMAP precipitation (January 1979–December 2010) is used to examine the Central American mid-summer drought. The International Satellite Cloud Climatology Project (ISSCP D2, Rossow et al. 1996) available from July 1983 through June 2006 is used to validate the simulated high, middle, and low cloud fraction. The Coordinated Ocean-ice Reference Experiments Phase 2 hindcast

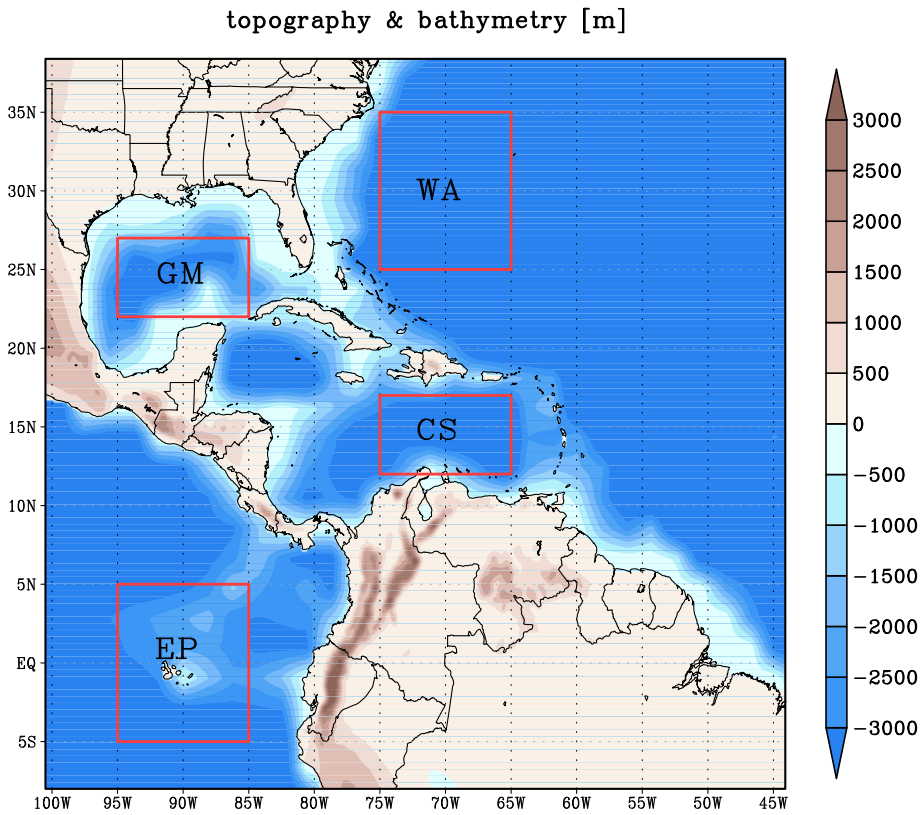

Fig. 1 Model domain, topography and bathymetry (m). The sub-domains of Gulf of Mexico (GM), Caribbean Sea (CS), Western Atlantic (WA) and Eastern Pacific (EP) are used for the subsequent analysis

Table 2 Observation list

Variable	Reference	Resolution	Platform	Acronym
Sea Surface Temperature	Reynolds et al. (2007)	0.25°	Satellite, in situ observation	NOAA
Wind sress	Risien and Chelton (2008)	0.25°	Quickscat sateliite	SCOW
925hpa wind	http://www.ncdc.noaa.gov/oa/climate/igra/	Station	Radiosonde	IGRA
Precipitation	Xie and Arkin (1997)	2.5°	Satellite, in situ observation	CMAP
Cloud	Rossow et al. 1996	2.5°	Satellite	ISCCP
Radiation	Large and Yeager (2009)	1°	Bulk formula simulation	COREII
Sea Surface Height	http://aviso.oceanobs.com	1°/3	Satellite	AVISO
Ocean heat content	Ingleby and Huddleston (2007)	1°	Objective analysis	EN3
Ocean surface current	Bonjean and Lagerloef (2002)	1°/3	Satellite altimeter and scatterometer	OSCAR

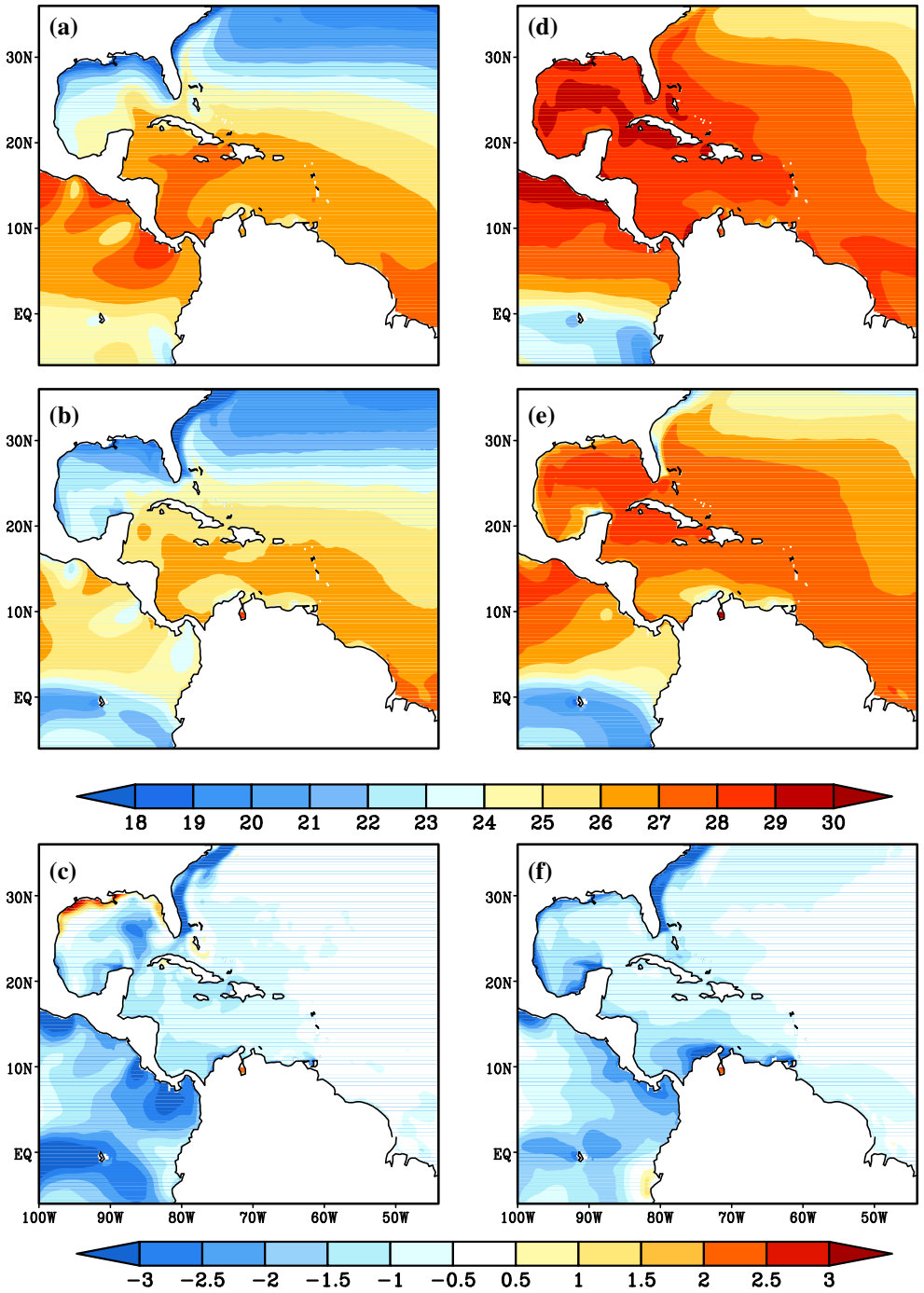

Fig. 2 DJF SST climatology (°C) from **a** observation, **b** ROARS and **c** the difference between ROARS and observation; JJA SST climatology from **d** observation, **e** ROARS and **f** the difference between ROARS and observation

simulations (COREII, Large and Yeager 2009) are used to validate the atmospheric fluxes.

The SST is the daily OI SST (Reynolds et al. 2007), which includes the AVHRR-only product version 1 (November 1981–May 2002) and the AMSR + AVHRR product version 2 (after June 2002). The CFSR is also strongly nudged to this daily OI SST, which is abbreviated NOAA SST hereafter. The AVISO Altimetry (available from 1993 to 2009) (http://aviso.oceanobs.com) is used to validate the Sea Surface Height (SSH). The upper 300 m averaged ocean temperature of the EN3 from the Met Office (Ingleby and Huddleston 2007) is

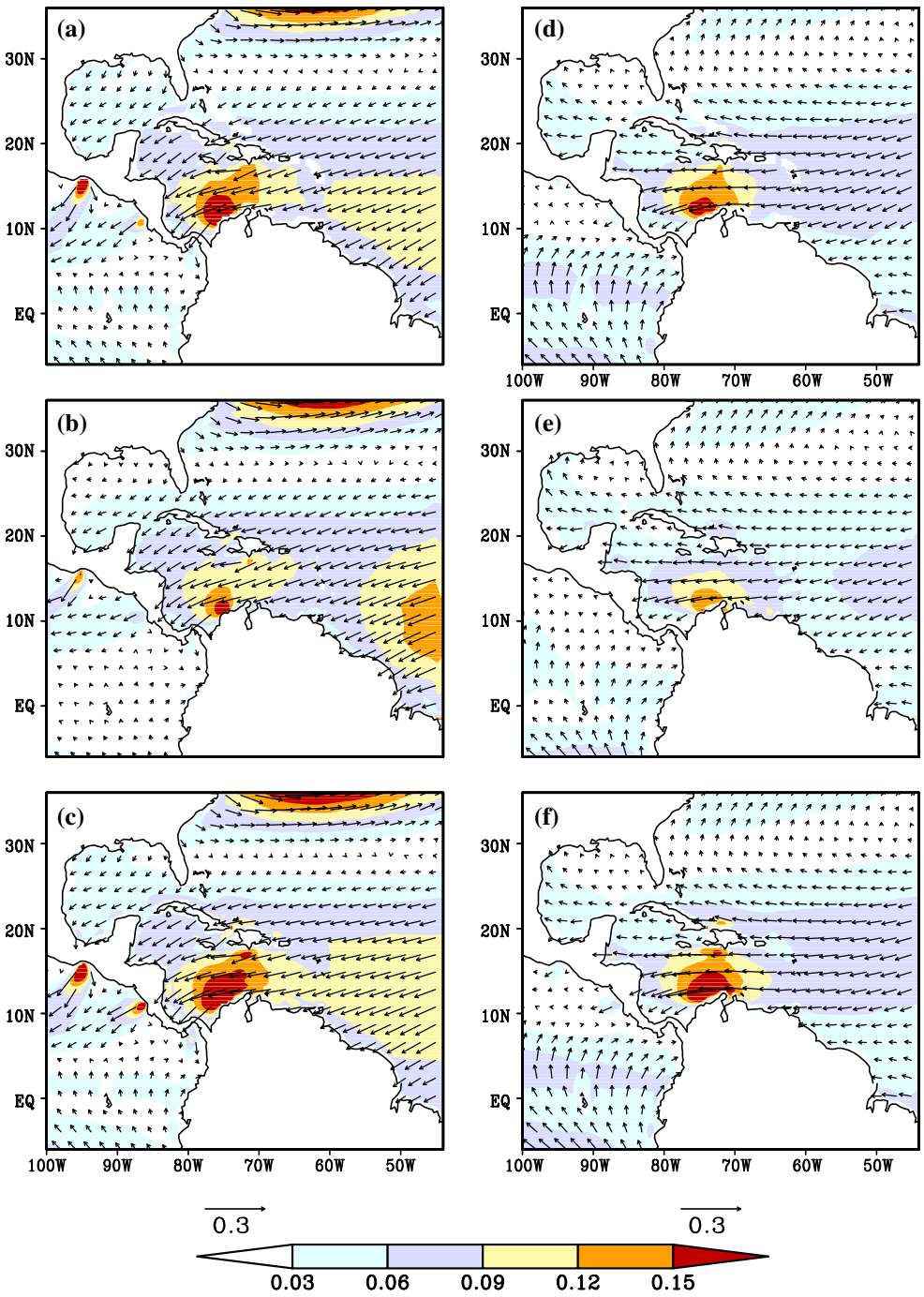

Fig. 3 The wind stress climatology (N/m^2) in DJF from **a** SCOW observation, **b** ROARS simulation, **c** CFSR, and in JJA from **d** SCOW observation, **e** ROARS simulation, and **f** CFSR

used to validate the Ocean Heat Content (OHC). The Ocean Surface Current Analysis—Real time (OSCAR, Bonjean and Lagerloef 2002) is a near-real time global ocean surface currents analysis derived from satellite altimeter and scatterometer data. OSCAR is available since 1993, and is used to validate the ocean surface currents. The reference, resolution, platform and acronym of these observed variables are listed in table 2. All of these observational data were interpolated to 15 km grid of ROARS for validation of the simulation.

3.2 CFSR

The new CFSR (Saha et al. 2010) is a state-of-the-art coupled high resolution global NCEP Reanalysis for atmosphere, ocean, land and sea ice. The atmospheric

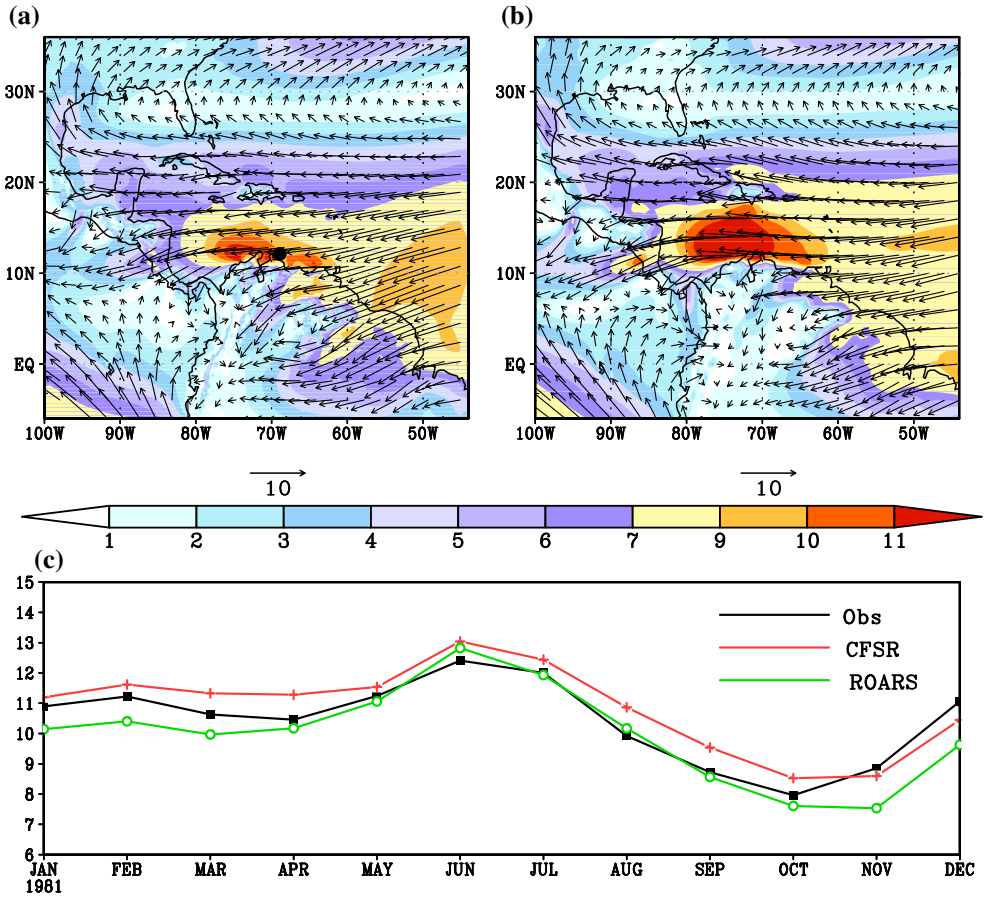

Fig. 4 Annual climatology of 925 hPa wind speed from **a** ROARS and **b** CFSR. **c** The annual cycle climatology of 925 hPa wind speed over Plesman Field (68.97°W, 12.2°N) from radiosonde (*black*), CFSR (*red*) and ROARS (*green*)

component of CFSR is the Global Forecast System (GFS) with much higher horizontal and vertical resolution (T382L64). The ocean component of CFSR is the GFDL MOM version 4p0d (MOM4) (Griffies et al. 2004). The zonal resolution of MOM4 is 0.5°, and the meridional resolution is 0.25° between 10°S and 10°N, gradually increasing from the tropics to 0.5° poleward of 30°S and 30°N. There are 40 vertical layers in the MOM4. It is noted that the IAS region is in the range of 10°N and 30°N. In a vein of being inclusive of an interactive physical climate system, the CFSR was promoted as a first step towards a coupled ocean–atmosphere global reanalysis (Saha et al. 2010). In CFSR although a global coupled ocean–atmosphere model was used to generate the first guess field for the data assimilation cycle, the observations were actually assimilated in the individual uncoupled models of land, ocean, sea-ice, and atmosphere. The CFSR with this attempt has provided a one-stop resource of analyzed variables of atmosphere, land, and oceanic variables, which makes holistic diagnosis of the physical climate system easier.

4 Results

4.1 Climatology

4.1.1 SST

The observed SST climatology is shown in Fig. 2 for the two contrasting seasons December–January–February (DJF) and June–July–August (JJA; for brevity other seasons are excluded). In both the seasons ROARS exhibits a cold bias that is most severe in the coastal regions, while in the open oceans the bias is comparatively far less. However in the DJF season the US Gulf coast exhibits a warm bias. It should be noted that ROARS does not use any heat flux correction during the integration period and therefore this relatively low SST bias in the open oceans is a reflection of the fidelity of the ROARS. Since ROARS is a coupled ocean–atmosphere integration, the relatively low SST bias is also a reflection of the atmospheric variability, especially of the low level winds in the summer time when the wind driven evaporation from the easterly flow of the southern flank of the North American subtropical high is significant

(Misra et al. 2009). Along the coastlines however it is far more difficult to verify especially when there is a mismatch in resolution between the observed product (at 0.25°) and ROARS (at 15 km ~0.14°). Furthermore, RSM–ROMS does not include the fresh water discharge from the river mouths along the coast and the relatively coarse vertical resolution in the mixed layer in ROMS for resolving the coastal processes could be other potential issues affecting the SST simulation in ROARS along the coastlines.

4.1.2 Wind stress

The wind stress climatology in DJF and the corresponding analysis from ROARS simulation and CFSR are shown in Figs. 3a, b, and c respectively. The superiority of CFSR's

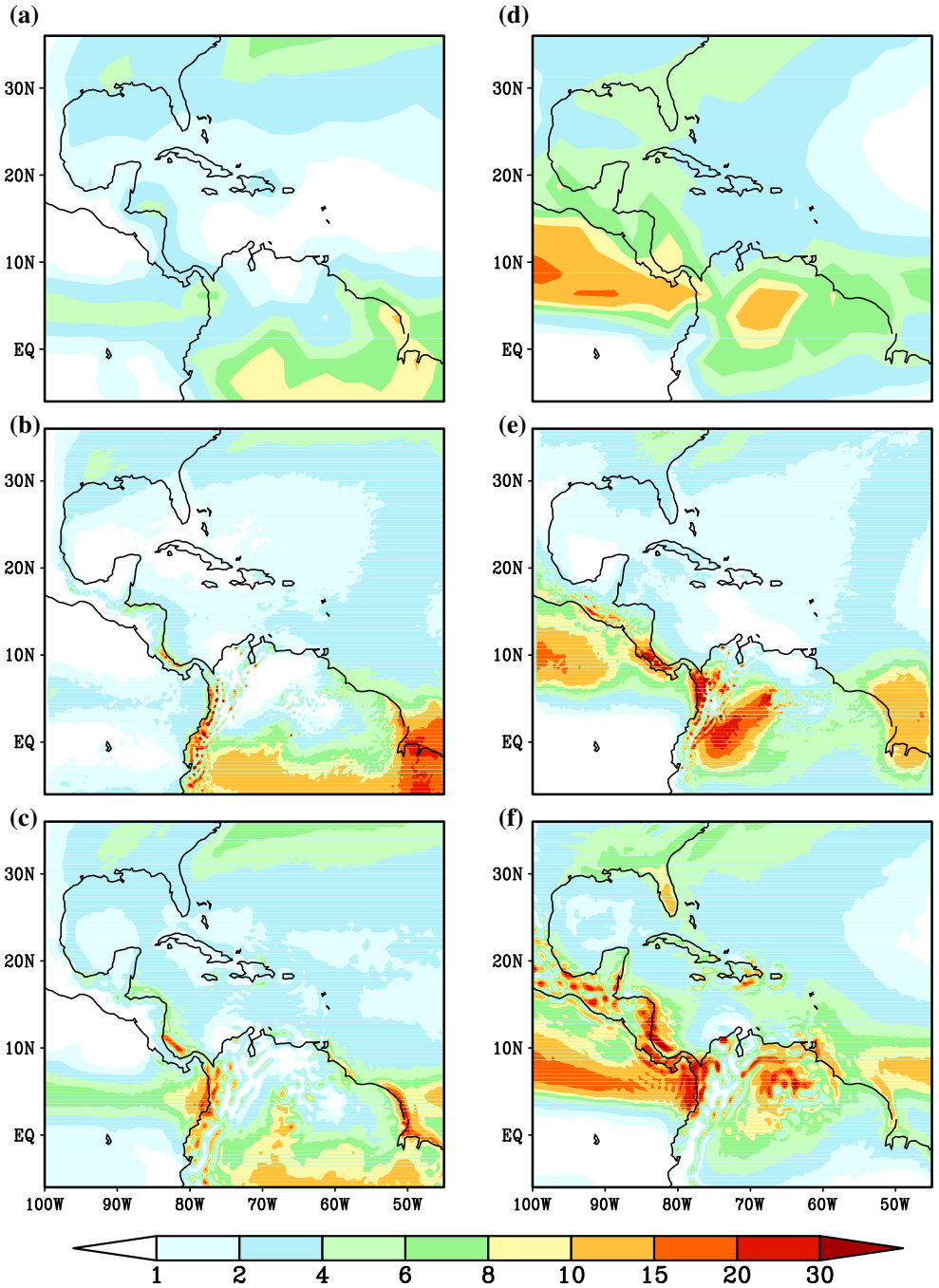

Fig. 5 DJF precipitation climatology (mm/day) from **a** CMAP observation, **b** ROARS simulation, and **c** CFSR; JJA precipitation climatology (mm/day) from **d** CMAP observation, **e** ROARS simulation, and **f** CFSR

verification (Fig. 3c) with SCOW observations in Fig. 3a over the ROARS simulation (Fig. 3b) is apparent. The easterly bias in the tropical Atlantic especially along the eastern lateral edge of the ROARS domain and the westerly bias along the coasts of Colombia and Venezuela in ROARS are some of the most prominent differences from the CFSR. Similarly in the summer season (JJA), the bias in the wind stress is comparatively higher in ROARS (Fig. 3e) compared to CFSR (Fig. 3f). However in comparison to the DJF season, the easterly bias in the eastern part of the domain and the westerly bias over the northern coasts of Venezuela and Colombia in ROARS are far less in the JJA season.

4.1.3 925 hPa winds

Figure 4 shows the annual mean climatology of 925 hPa winds from ROARS and CFSR. The Caribbean Low Level Jet (CLLJ) is seen as winds in excess of 10 ms^{-1} at 925 hPa that has a bi-annual peak along the northern coast of Colombia and Venezuela, peaking in the boreal summer and winter seasons. The CLLJ from ROARS and CFSR is verified with corresponding 925 hPa monthly wind climatology from IGRA radiosonde data over Plesman Field (indicated by the black dot in Fig. 4a and located at 68.97°W and 12.2°N). It is seen that the depiction of CLLJ over Plesman field in both the CFSR and ROARS is reasonable. The seasonal peak in June followed by that in December is also well picked in both CFSR and ROARS. However further west of Plesman Field, the CLLJ in ROARS is weaker than that in CFSR. But outside of the CLLJ region, the annual mean climatology of easterly winds over the Caribbean Sea and the northern tropical Atlantic are comparable in ROARS and CFSR.

4.1.4 Precipitation

The precipitation climatology for the winter and summer seasons are shown in Fig. 5. The relatively dry IAS and northern part of South America (e.g. Venezuela, northern Colombia) in ROARS (Fig. 5b) is comparable to that in CMAP observations (Fig. 5a) during the DJF season. The corresponding DJF rainfall climatology in CFSR (Fig. 5c) has a higher wet bias. Similarly the DJF rainfall climatology over southeastern US in ROARS and CFSR are reasonable in comparison to the corresponding observed climatology. However both ROARS and CFSR show

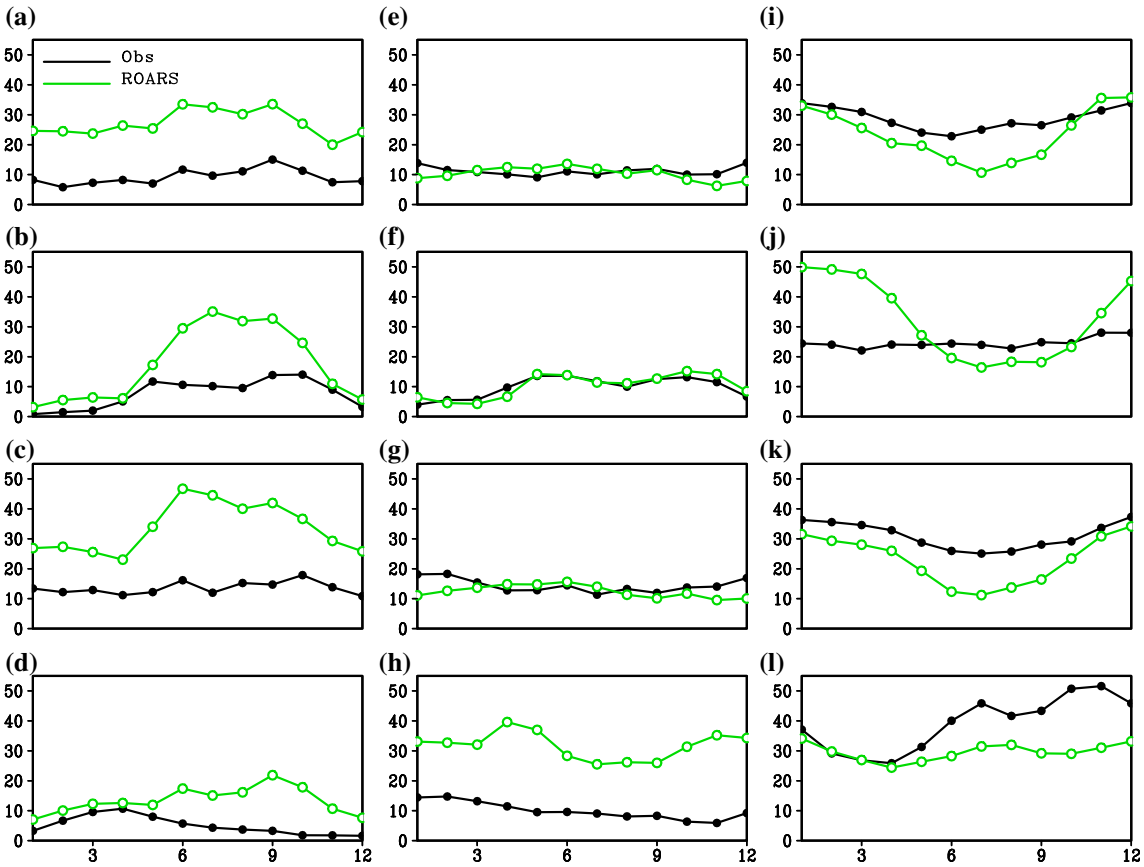

Fig. 6 The annual cycle climatology of high cloud cover fraction (%) over **a** Gulf of Mexico, **b** Caribbean Sea, **c** Western Atlantic and **d** Eastern Pacific; **e**–**h** are for middle cloud; **i**–**l** are for low cloud. ISCCP observation is in *black*, and the ROARS simulation is in *green*

significant wet bias in DJF over central Brazil near the southern boundary of the domain. Furthermore ROARS (CFSR) shows a dry (wet) bias in DJF over eastern equatorial Pacific Ocean. In the summer season (JJA) both ROARS (Fig. 5e) and CFSR (Fig. 5f) show larger disagreement with CMAP observations (Fig. 5d) than in the DJF season especially over land. However the general observed pattern of relatively less rainfall over the IAS compared to that over the neighboring land regions is maintained in both ROARS and CFSR. But the wet bias over Central America and northern part of South America in both ROARS and CFSR is apparent. In addition the dry bias over southeastern U.S. and IAS in ROARS is in contrast to the wet bias in CFSR. The cold SST bias of ROARS over the Eastern Pacific, Caribbean Sea and Gulf of Mexico results in the underestimation of precipitation in winter and summer.

4.1.5 Clouds and radiation

In Fig. 6 we show the seasonal cycle of high, middle, and low clouds over the Gulf of Mexico, Caribbean Sea, Western Atlantic, and Eastern Pacific Oceans (see Fig. 1 for their domain locations) from ROARS and corresponding ISCCP observations. It is quite apparent from the figure that the middle clouds verify the best relative to high and low clouds except over the eastern Pacific Ocean. In fact the verification of the total clouds in the

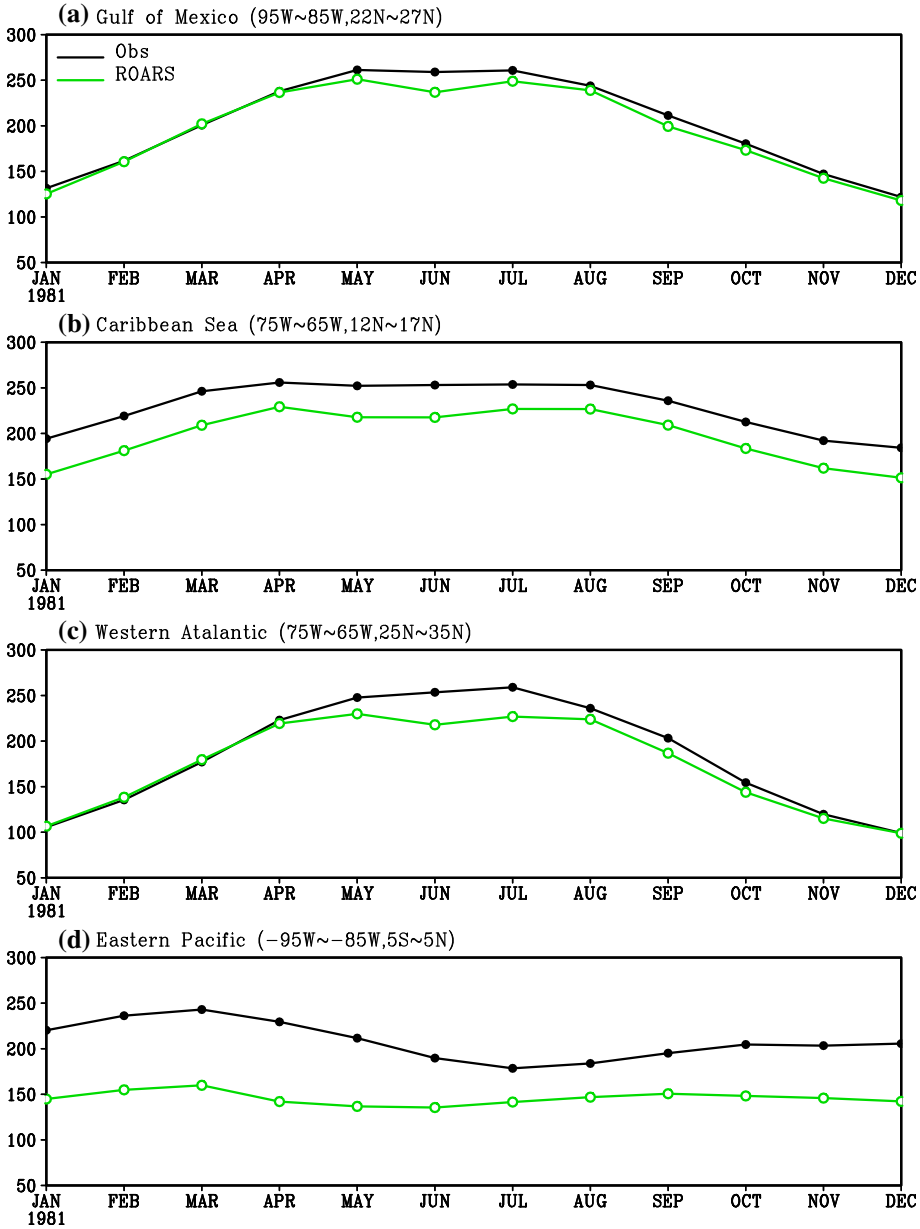

Fig. 7 The annual cycle climatology of net short wave radiation (W/m^2) over **a** Gulf of Mexico, **b** Caribbean Sea, **c** Western Atlantic and **d** Eastern Pacific. COREII observation is in *black*, and the ROARS simulation is in *green*

column in these four oceanic regions is most reasonable relative to low, middle, and high clouds (not shown). In the case of high clouds, ROARS exhibits a bias of excess cloud fraction throughout the year in all four of the oceanic regions with the bias peaking in the boreal summer season and gradually reducing into the fall season. The bias in the low level clouds in ROARS is relatively less than that in the high clouds with the Gulf of Mexico exhibiting the least of all the other three oceanic regions. In addition except for the Caribbean region in late boreal fall and winter seasons, ROARS tend to underestimate the low level cloud fraction in the rest of the oceanic regions. Misra and DiNapoli (2012) in their observational study suggested that the downwelling shortwave flux is one of the most important surface heat flux terms in the boreal summer and fall seasons that regulate the SST in IAS. Therefore we examine the bias in the shortwave flux in Fig. 7, which shows that ROARS exhibits an underestimation of the downwelling shortwave flux at surface especially in the summer and fall seasons over the western Atlantic and Gulf of Mexico region, while it is underestimated throughout the year over the Caribbean Sea and in the eastern Pacific Ocean. This underestimation of shortwave flux is coincident with the corresponding excess bias of the high (middle) cloud fraction over the Caribbean Sea (eastern Pacific; Fig. 7). Over Gulf of Mexico and western Atlantic Ocean the cloud bias (Fig. 6) and shortwave bias (Fig. 7) is relatively smaller than the other two oceanic regions.

4.2 Interannual variability

4.2.1 Sea Surface Height (SSH)

The standard deviation of the SSH from observations, ROARS, and CFSR was shown in Fig. 8. The SSH data was not assimilated in the CFSR (Xue et al. 2011), and the CFSR (Fig. 8c) exhibits very little variability compared to the observations (Fig. 8a) over the IAS region. In contrast ROARS (Fig. 8b) is able to capture the variance of the SSH over the Gulf of Mexico, the Caribbean Sea, and the northwestern Atlantic Ocean, although this variance is overestimated in ROARS relative to the observation. This variability in the SSH in the observations and ROARS is a reflection of the corresponding variability in the ocean circulation and ocean heat storage over these regions.

4.2.2 Sea surface temperature (SST)

Figure 9 show the time series of the area averaged SST anomaly over the Gulf of Mexico, Caribbean Sea,

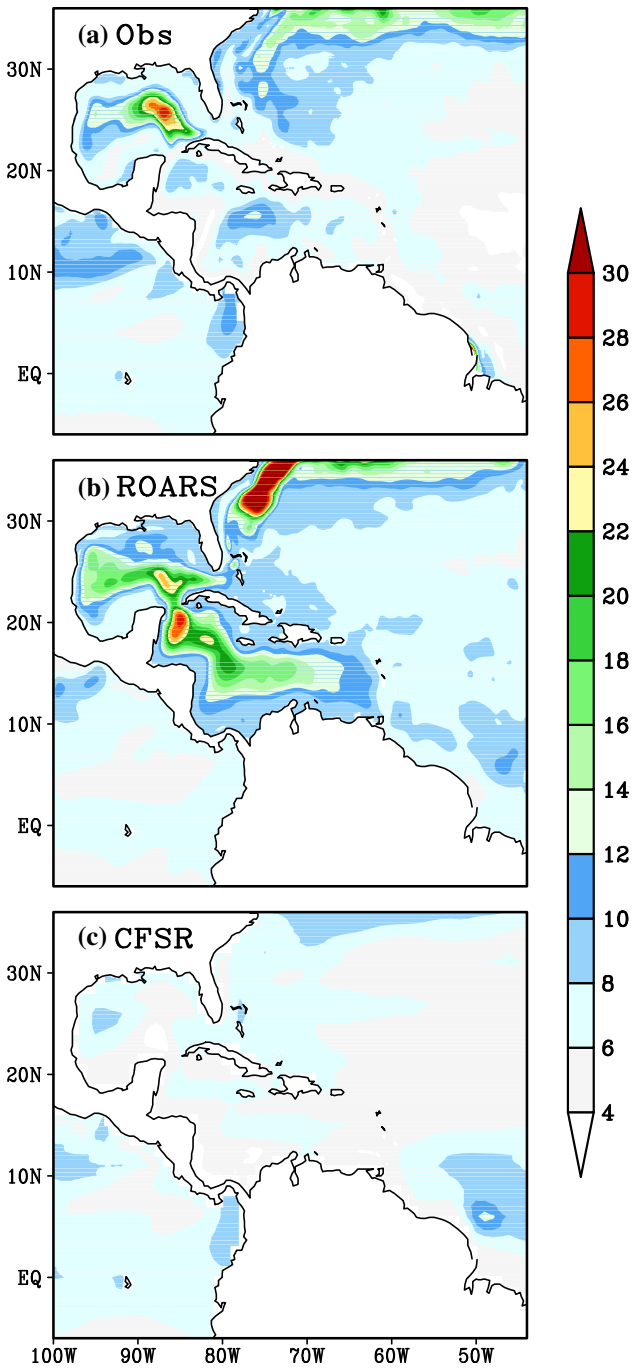

Fig. 8 Monthly Sea Surface Height standard deviation (cm) from **a** AVHRR observation, **b** ROARS simulation, and **c** CFSR

western Atlantic, and eastern Pacific from observations and ROARS. It should be noted that in CFSR there is a strong relaxation of the SST towards the observed daily NOAA SST through the period of the reanalysis while in ROARS there is no such heat flux correction being used. Thus the ROARS SST variability is only compared with observation. The standard deviation of SST over Gulf of Mexico (Fig. 9a) from observation and ROARS

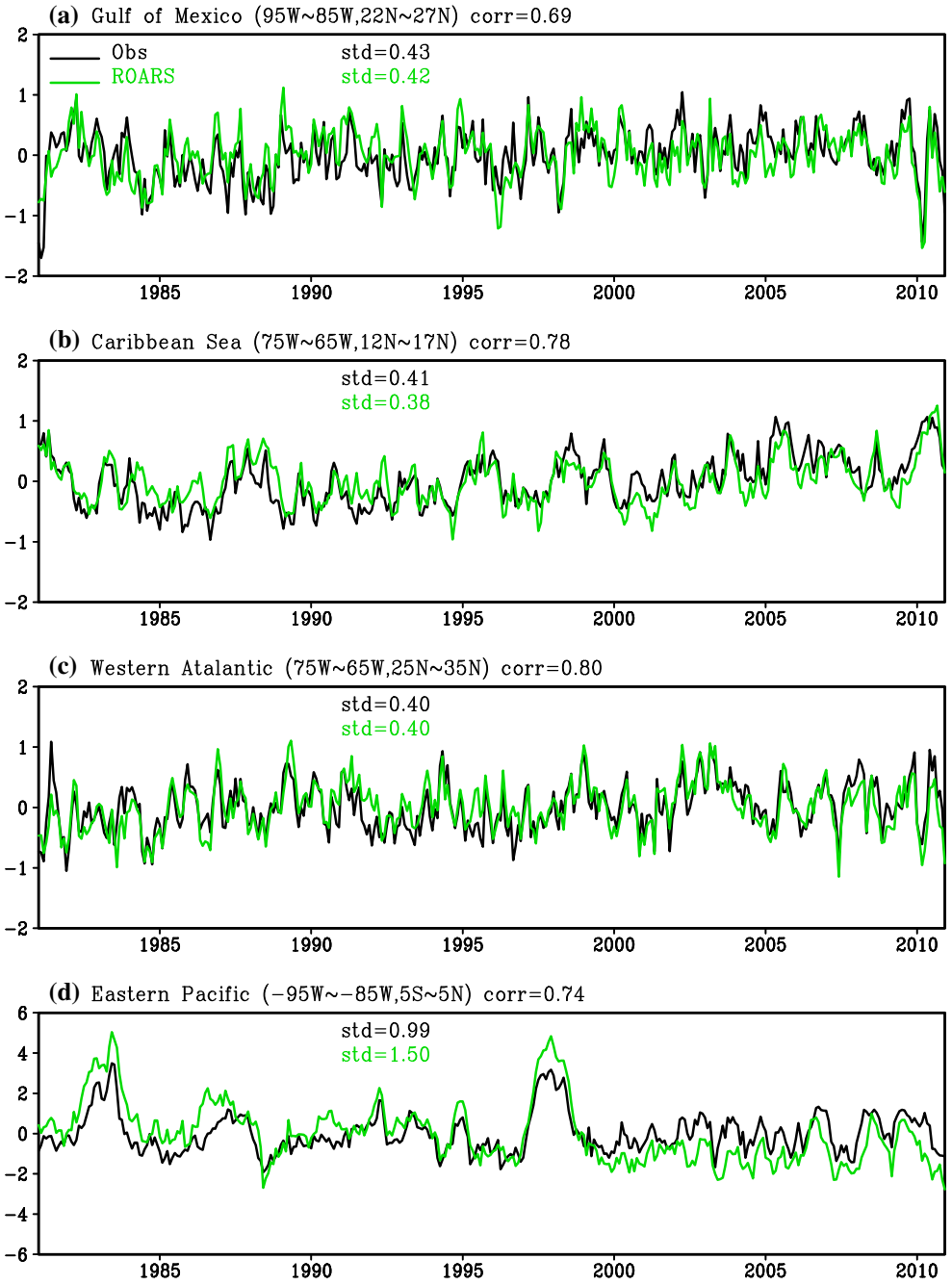

Fig. 9 Monthly SST anomaly (°C) over **a** Gulf of Mexico, **b** Caribbean Sea, **c** Western Atlantic and **d** Eastern Pacific. Observation is in *black*, and the ROARS simulation is in *green*

simulation is 0.43 and 0.42 °C respectively, and the correlation between them is 0.69. The standard deviation of SST over Caribbean Sea (Fig. 9b) is 0.41 and 0.38 °C for observation and ROARS simulation respectively, and the correlation between them is 0.78. The SD of SST over Western Atlantic (Fig. 9c) is 0.40 °C for both observation and ROARS, and the correlation between them is as high as 0.80. The SST standard deviation is largest over Eastern Pacific (Fig. 9d) than over other domains, and the temporal correlation is 0.74.

4.2.3 Ocean heat content (OHC)

The OHC is represented by the upper 300 m ocean temperature as in Xue et al. (2011). The time series of the area averaged ocean heat content over the 4 oceanic regions are

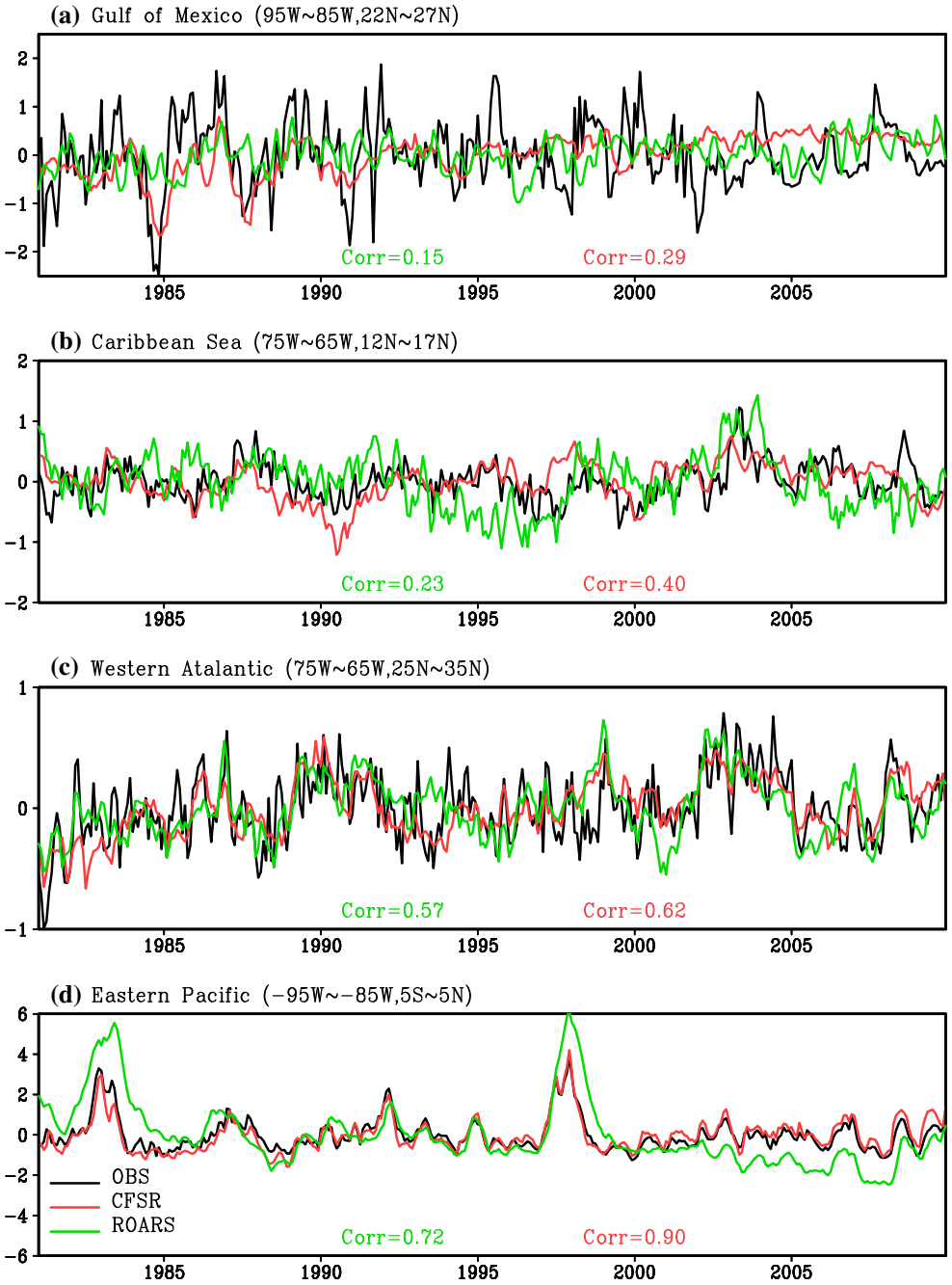

Fig. 10 Monthly Ocean Heat Content anomaly (°C) over **a** Gulf of Mexico, **b** Caribbean Sea, **c** Western Atlantic and **d** Eastern Pacific. EN3 analysis observation is in *black*, the ROARS simulation is in *green*, and CFSR is in *red*

shown in Fig. 10 from ROARS, CFSR, and corresponding EN3 analysis. Since the CFSR SST was strongly nudged to the NOAA daily OISST, the OHC from CFSR verifies with observation better than ROARS. The positive correlations in both reanalysis products ROARS (and CFSR) are highest over the eastern equatorial Pacific 0.72 (and 0.90) followed by that over western Atlantic 0.57 (and 0.62), Caribbean Sea 0.23 (and 0.40) and Gulf of Mexico 0.15 (and 0.29).

4.2.4 Precipitation

Similarly the time series of area-averaged precipitation over the four oceanic regions are shown in Fig. 11. In all four regions we observe that the positive correlations of precipitation from CFSR with corresponding observations are higher relative to ROARS. We find in ROARS the highest correlation is over eastern Pacific Ocean (0.78)

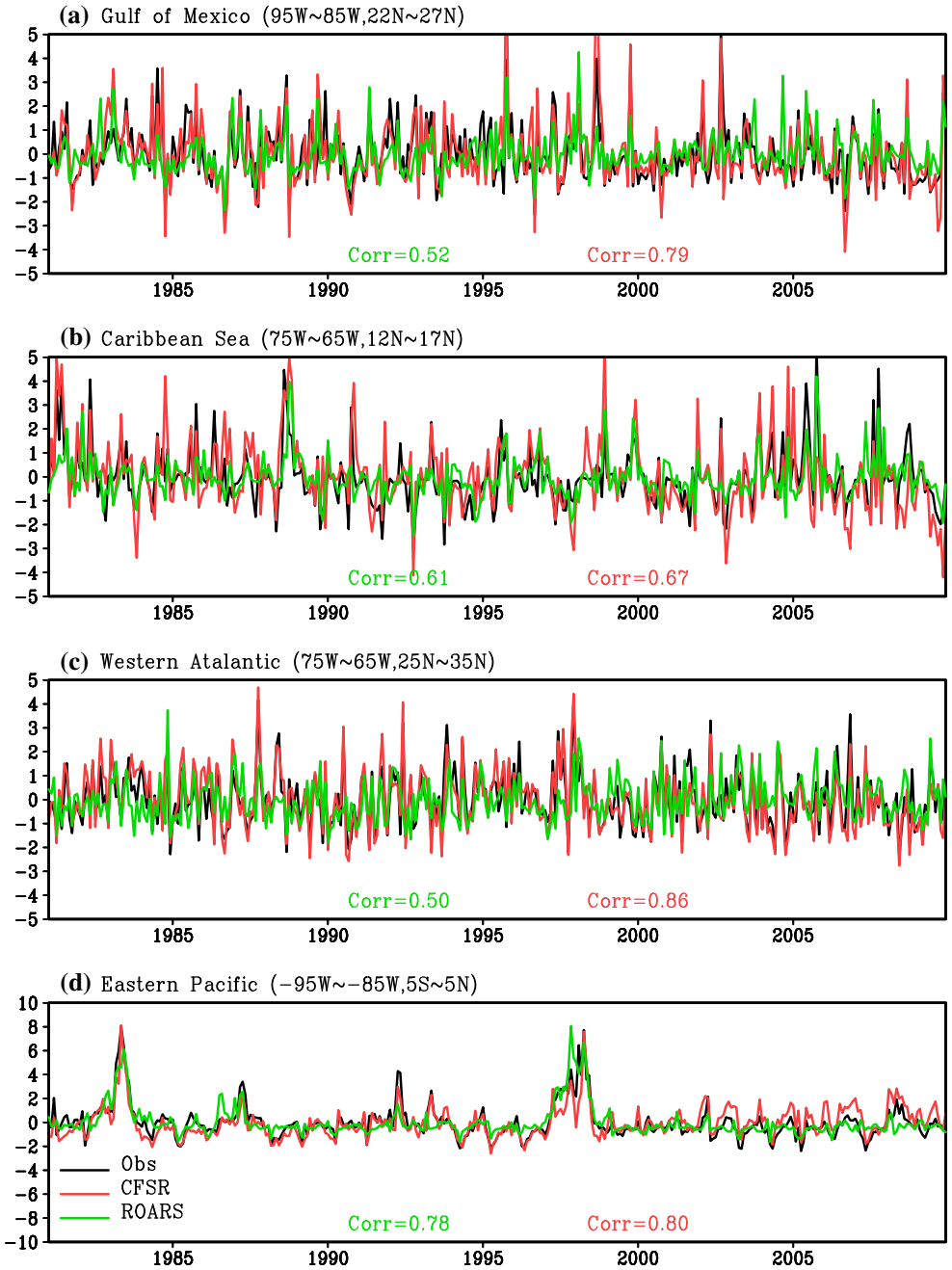

Fig. 11 The monthly precipitation anomaly (mm/day) over **a** Gulf of Mexico, **b** Caribbean Sea, **c** Western Atlantic and **d** Eastern Pacific. The CMAP observation is in *black*, the ROARS simulation is in *green*, and CFSR is in *red*

followed by that over the Caribbean Sea (0.61). Over the Gulf of Mexico (0.52) and the western Atlantic (0.50) the correlations of rainfall variability in ROARS is comparable and smaller than the other two oceanic regions. In CFSR however the correlations are highest in the Western Atlantic (0.86) and is followed by that over eastern Pacific Ocean (0.80), the Gulf of Mexico (0.79), and the least is over the Caribbean Sea (0.67). Over the entire domain in Fig. 1 the correlation of ROARS is 0.69, and the correlation of CFSR precipitation is 0.79.

4.2.5 Relationship with ENSO variations

The ENSO teleconnections on the winter season (DJF) rainfall over the domain is well known (Ropelewski and Halpert 1987; Kiladis and Diaz 1989; Diaz et al. 2001).

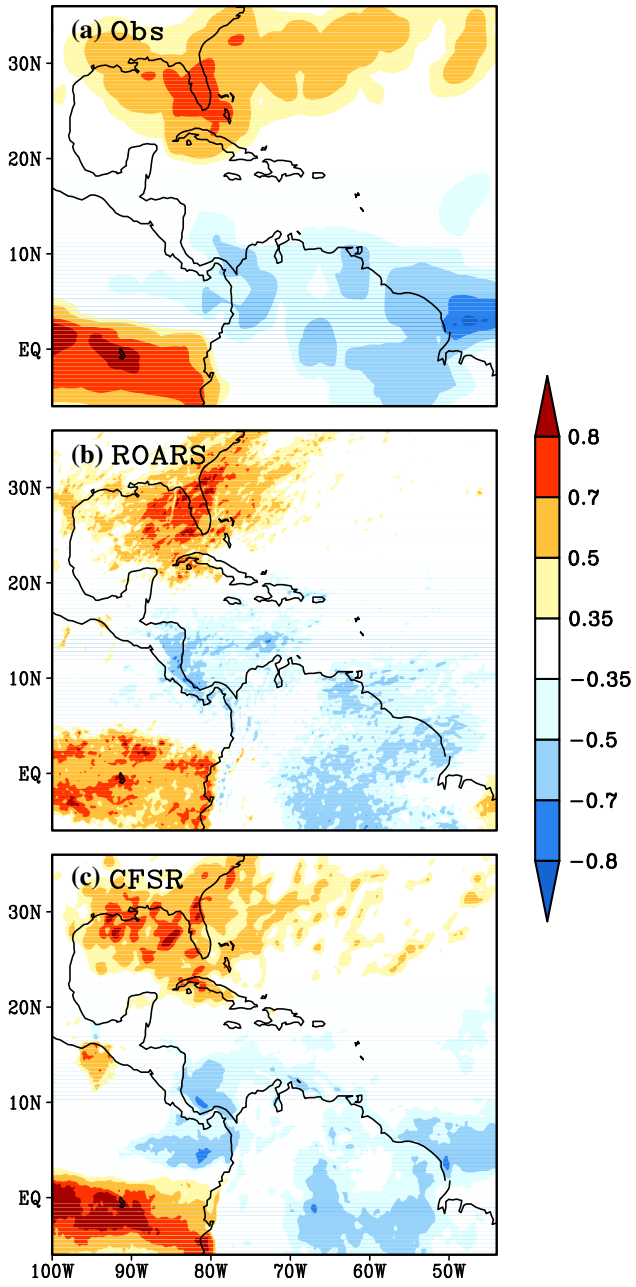

Fig. 12 The correlation of DJF SST against precipitation over (100°W–85°W, 5°S–5°N) from **a** observation, **b** ROARS, and **c** CFSR. The correlation with 5 % significant level of Student's test is *shaded*

Since the ROARS domain does not completely cover the Niño3 region (150°W–90°W; 5°S–5°N) we have used an alternative ENSO SST index averaged over 100°W–85°W and 5°S–5°N to examine the ENSO teleconnections on the winter rainfall in Fig. 12. It is apparent from the figure that ROARS and CFSR are able to capture the observed robust teleconnections over the southeastern US and over tropical South America while the local observed positive correlations over the eastern equatorial Pacific is also simulated by both ROARS and CFSR.

4.3 Phenomenological features

4.3.1 Ocean circulation

A characteristic feature of the ocean circulation in this domain is the loop current and eddies that are generated off this current periodically. A winter month of January 2000 and a summer month of July 2000 are arbitrarily selected to examine this feature. In January 2000 we isolated one such example of loop current shedding an eddy that is captured in ROARS (Fig. 13b). In CFSR (Fig. 13c) the loop current is barely simulated while the eddies in the western Gulf of Mexico are not simulated at all. The eddies typically persist beyond 6 months and in July 2000 we continue to see the eddies in the western Gulf of Mexico both in observations (Fig. 13d) and ROARS (Fig. 13e) while CFSR (Fig. 13f) remains quiescent. The ROARS surface current is much stronger than observation over Caribbean Sea, Gulf of Mexico and the U.S. eastern coast (Gulf Stream). This is consistent with the stronger ROARS SSH variance in Fig. 8. It may however be noted that the location of the eddies in ROARS do not exactly match with that in observations. It is shown that the ocean model of CFSR with a low resolution of about 0.5° over IAS is barely able resolve the Loop Current and completely misses the eddy shedding.

4.3.2 Mid-summer drought

The mid-summer drought is a unique phenomenon that is wide spread across the North American monsoon region and the Caribbean (Hastenrath 1967; Magana et al. 1999). Hastenrath (2002) claims that this phenomenon is caused by the meridional movement of the ITCZ over the Central American region. In contrast Magana et al. (1999) suggest that the mid-summer drought is caused by coupled air–sea interactions in the neighboring oceans of Central America. On the other hand several studies indicate that subsidence induced by intensification and expansion of the north Atlantic subtropical high leads to the mid-summer drought in the region (Hastenrath 1976, 1978, 1984; Granger 1985; Giannini et al. 2000). The mid-summer drought is characterized by a subtle but significant reduction of monthly mean rainfall in July relative to June and August. We examine this feature over Central America (98°W–83°W and 10°N–20°N; Fig. 14). It is seen from the figure that both ROARS and CFSR overestimate this phenomenon by overestimating the rainfall in June and August over Central America relative to the observations. The relative dip in July rainfall climatology

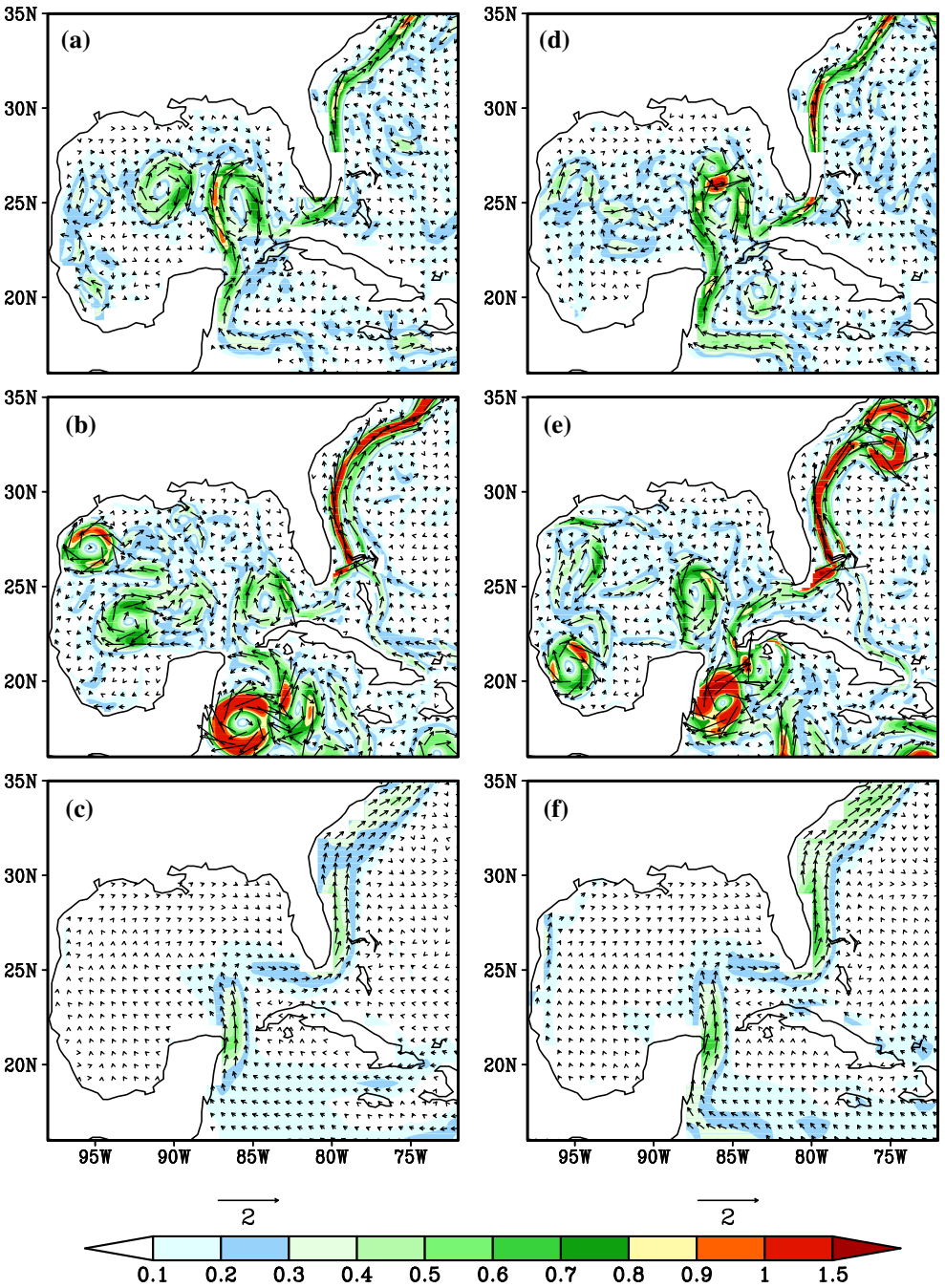

Fig. 13 The ocean surface current (m/s) in January 2000 from **a** OSCAR satellite observation, **b** ROARS simulation, **c** CFSR, and in July 2000 from **d** OSCAR satellite observation, **e** ROARS simulation, and **f** CFSR

over Central America (Fig. 14) is comparable to observations in ROARS while CFSR continues to have the wet bias.

5 Conclusions

In this paper we have extensively verified a multi-decadal integration of a regional ocean–atmosphere coupled model (RSM–ROMS) forced by NCEP R-2 global atmospheric reanalysis and SODA ocean reanalysis, which we refer as ROARS (Regional Ocean–Atmosphere coupled downscaling of global Reanalysis over the Intra-American Seas). No explicit flux correction is applied during this coupled integration, which is conducted at approximately 15 km grid resolution covering a relatively large extending from 100.49°W–44.097°W to 8.002°S–38.391°N. This high-resolution coupled downscaling was conducted to examine

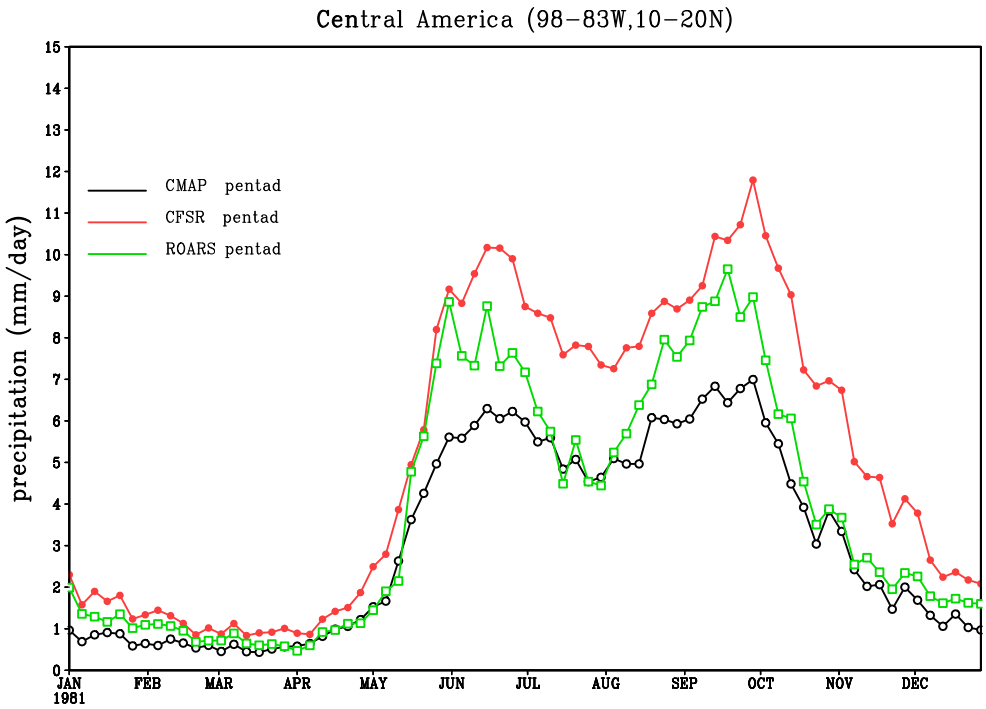

Fig. 14 The pentad precipitation climatology (mm/day) over Central America (98°–83°W, 10°–20°N) from CMAP (*black*), ROARS (*green*) and CFSR (*red*)

the capability of RSM–ROMS over IAS prior to the coupled downscaling of seasonal forecast and CMIP5 decadal hindcasts and climate change projection.

We have used a variety of variables including SST, low level atmospheric winds, sea surface height, precipitation, ocean surface currents, cloud cover, downwelling shortwave flux at surface, wind stress, ocean heat content to verify against corresponding observations and compare with the recently released CFSR (Saha et al. 2010). The observations were obtained from diverse platforms including satellite based, independent data analysis (COREII), in situ observations of radiosondes and multisensor analysis (e.g. precipitation and SST analysis). A major difference between CFSR and ROARS besides the fact that former is global while the latter is regional is that unlike CFSR, ROARS does not explicitly employ any heat flux correction in the simulation of SST and nor does it assimilate any observations during its multi-decadal integrations.

ROARS reasonably reproduced the observed climatological spatial distribution of SST, near surface winds, and precipitation. However, our analysis reveals that ROARS exhibits a cold SST bias in the IAS region and over eastern equatorial Pacific Ocean both in the boreal summer and winter season. In the summer it is likely related to the excessive high clouds that tend to reduce the downwelling short wave flux at surface, which tends to be a dominant driver of SST in the IAS region (Misra and DiNapoli 2013). The lower tropospheric winds in the IAS region is characterized by the Caribbean low level jet that has a distinct seasonal cycle, which is reasonably well captured both in ROARS and CFSR when compared with in situ radiosonde observations. The underestimation of ROARS precipitation over the ITCZ and IAS region is most likely related to the cold SST bias from ROARS.

ROARS captures the variance of the SSH over the Caribbean Sea, Gulf of Mexico and the northwestern Atlantic as observation, while these SSH variance is very weak in the CFSR without the assimilation of altimetry SSH data. The ROARS simulated SST anomaly variance matches the observed SST very well. The correlation of ROARS SST is above 0.69 against observation over the four sub-domains of Caribbean Sea, Gulf of Mexico, Eastern Pacific and Western Atlantic. Both ROARS and CFSR reasonably simulates the observed OHC variability over Eastern Pacific and Western Atlantic than over Caribbean Sea and Gulf of Mexico. However, CFSR performs slightly better than ROARS over these sub-regions due to the assimilation of upper layer ocean temperature in the former. Although the correlation of ROARS precipitation against CMAP is lower than the CFSR, the correlation is still above 0.5 over the four sub-domains.

A highlight of ROARS is that with its relatively high resolution it is able to capture the complex ocean surface

currents including the loop current and eddy shedding off of it that is reflected in the variance of the sea surface height as well. In contrast, the CFSR with a resolution of about 0.5° over IAS is not able to capture these features. Another important feature of this region relates to the mid-summer drought in Central America, which is reasonably well captured by both ROARS and CFSR, with the wet bias in the former relatively lower than that in the latter.

In fact our comparisons between ROARS and CFSR indicate some inconsistencies in the latter. For example, the loop current and the eddies are considered to be critical mechanisms for the redistribution of the heat brought in from the Caribbean Sea throughout the Gulf of Mexico, especially in the western part of the Gulf (Chang and Oey 2010). However despite the poor rendition of these surface ocean features CFSR displays the observed SST and a comparatively much lower correlation of the OHC (0.29; Fig. 10a) over the Gulf of Mexico. In case of ROARS the bias in SST (Fig. 2) and OHC is apparent (Fig. 10), which is likely dominated by the bias in the clouds (Figs. 6, 7).

In summary ROARS does provide an alternative avenue to generate high resolution analysis of ocean and atmospheric climate over the IAS region, one of the most poorly observed region of the planet.

Acknowledgments This work was supported by grants from NOAA (NA12OAR4310078, NA10OAR4310215, NA11OAR4310110), and USDA (027865). Supercomputing was provided by TACC via XSEDE. Two anonymous reviewers helped to improve the manuscript.

References

Alpert JC, Kanamitsu M, Caplan PM, Sela JG, White G, Kalnay E (1988) Mountain induced gravity wave drag parameterization in the NMC medium-range model. Preprints, eighth conference on numerical weather prediction, Baltimore, MD. Amer Meteor Soc, pp 726–733

Amador JA (2008) The Intra-Americas Sea Low Level Jet (IALLJ): overview and future research, trends, and directions in climate research. Ann N Y Acad Sci 1146:153–188

Bonjean F, Lagerloef GSE (2002) Diagnostic model and analysis of the surface currents in the tropical Pacific Ocean. J Phys Oceanogr 32:2938–2954

Bosart LF, Lin SC (1984) A diagnostic analysis of the Presidents' Day storm of February 1979. Mon Weather Rev 112:2148–2177

Bosilovich MG, Schubert SD (2002) Water vapor tracers as diagnostics of the regional hydrologic cycle. J Hydrom 3:149–165

Carton JA, Chepurin G, Cao X, Giese BS (2000) A Simple Ocean Data Assimilation analysis of the global upper ocean 1950–1995, Part I: methodology. J Phys Oceanogr 30:294–309

Chan S, Misra V (2010) A diagnosis of the 1979–2005 extreme rainfall events in the southeastern United States with Isentropic Moisture Tracing. Mon Weather Rev 138:1172–1185

Chang Y-L, Oey L-Y (2010) Eddy and wind-forced heat transports in the Gulf of Mexico. J Phys Oceanogr 40:2728–2742

Chassignet EP, Hulburt HE, Smedstad OM, Barron CN, Ko DS, Rhodes RC, Shriver JF, Wallcraft AJ, Arnone AR (2005) Assessment of data assimilative ocean models in the Gulf of Mexico using Ocean Color. Circ Gulf Mex Obs Models 161:87–100

Chérubin LM, Sturges W, Chassignet EP (2005) Deep flow variability in the vicinity of the Yucatan Straits from a high-resolution MICOM simulation. J Geophys Res 110:C04009. doi:10.1029/2004JC002280

Chérubin LM, Morel Y, Chassignet EP (2006) Loop current ring shedding: the formation of cyclones and the effect of topography. J Phys Oceanogr 36:569–591

Chou M-D, Lee K-T (1996) Parameterizations for the absorption of solar radiation by water vapor and ozone. J Atmos Sci 53:1203–1208

Chou M-D, Suarez MJ (1994) An efficient thermal infrared radiation parameterization for use in general circulation models. Technical report series on global modeling and data assimilation, NASA/TM-1994-104606, 3, 85 pp

Diaz HF, Hoerling MP, Eischeid JK (2001) ENSO variability, teleconnections and climate change. Int J Climatol 21:1845–1862

Ek MB, Mitchell KE, Lin Y, Rogers E, Grunmann P, Koren V, Gayno G, Tarpley JD (2003) Implementation of Noah land surface model advances in the National Centers for Environmental Prediction operational mesoscale 437 Eta model. J Geophys Res 108:8851. doi:10.1029/2002JD003296

Giannini A, Kushnir Y, Cane MA (2000) Interannual variability of Caribbean rainfall, ENSO, and the Atlantic Ocean. J Clim 13:297–311

Granger OE (1985) Caribbean climates. Prog Phys Geogr 9(1):16–43

Haidvogel DB, Arango HG, Hedstrom K, Beckmann A, Malanotte-Rizzoli P, Shchepetkin AF (2000) Model evaluation experiments in the North Atlantic Basin: simulations in nonlinear terrain-following coordinates. Dyn Atmos Oceans 32:239–281

Hastenrath S (1967) Rainfall distribution and regime in Central America. Arch Meteor Geophys Bioklimatol 15B:201–241

Hastenrath S (1976) Variations in low-latitude circulation and extreme climatic events in the tropical Americas. J Atmos Sci 33:20–215

Hastenrath S (1978) On the modes of tropical circulation and anomalies. J Atmos Sci 35:22220–22231

Hastenrath S (1984) Interannual variability and annual cycle: mechanisms of circulation and climate in the tropical Atlantic sector. Mon Weather Rev 112:1097–1107

Hastenrath S (2002) The intertropical convergence zone of the Eastern Pacific revisited. Int J Climatol 22:347–356

Hong SY, Pan HL (1996) Nonlocal boundary layer vertical diffusion in a medium-range forecast model. Mon Weather Rev 124:2322–2339

Hurlburt HE, Thompson JD (1980) A numerical study of loop current intrusions and eddy shedding. J Phys Oceanogr 10:1611–1651

Hurrel JG, Meehl A, Bader D, Delworth TL, Kirtman B, Wielicki B (2009) A unified modeling approach to climate system prediction. Bull Am Meteorol Soc 90:1819–1832

Ingleby B, Huddleston M (2007) Quality control of ocean temperature and salinity profiles—historical and real-time data. J Mar Syst 65:158–175

Juang HMH, Kanamitsu M (1994) The NMC nested regional spectral model. Mon Weather Rev 122:3–26

Juang HMH, Hong SY, Kanamitsu M (1997) The NCEP regional spectral model: an update. Bull Am Meteorol Soc 78:2125–2143

Kanamaru H, Kanamitsu M (2007) Scale-selective bias correction in a downscaling of global reanalysis using a regional model. Mon Weather Rev 135:334–350

Kanamitsu M, Ebisuzaki W, Wollen J, Yang SK, Hnilo JJ, Fiorino M, Potter GL (2002) NCEP-DOE AMIP-II reanalysis. Bull Am Meteorol Soc 83:1631–1643

Kanamitsu M, Yoshimura K, Yhang Y, Hong S (2010) Errors of interannual variability and multi-decadal trend in dynamical regional climate downscaling and its corrections. J Geophys Res 115:D17115

Kiladis GN, Diaz HF (1989) Global climatic anomalies associated with extremes in the Southern Oscillation. J Clim 2:1069–1090

Large WG, Yeager SG (2009) The global climatology of an internationally varying air–sea flux data set. Clim Dyn 33:341–364

Li H, Kanamitsu M, Hong SY (2012) California reanalysis downscaling at 10 km using an ocean–atmosphere coupled regional model system. J Geophys Res 117:D12118. doi:10.1029/2011JD017372

Li H, Kanamitsu M, Hong SY, Yoshimura K, Cayan DR, Misra V (2013a) A high-resolution ocean–atmosphere coupled downscaling of a present climate over California. Clim Dyn. doi:10.1007/s00382-013-1670-7

Li H, Kanamitsu M, Hong SY, Yoshimura K, Cayan DR, Misra V, Sun L (2013b) Projected climate change scenario over California by a regional ocean–atmosphere coupled model system. Clim Change. doi:10.1007/s10584-013-1025-8

Liu Y, Lee S-K, Muhling BA, Lamkin JT, Enfield DB (2012) Significant reduction of the Loop Current in the 21st century and its impact on the Gulf of Mexico. J Geophys Res 117:C05039. doi:10.1029/2011JC007555

Magana V, Amador JA, Medina S (1999) The mid-summer drought over Mexico and Central America. J Clim 12:1577–1588

Mestas-Nuñez AM, Enfield DB, Zhang C (2007) Water vapor fluxes over the Intra-Americas Sea: seasonal and interannual variability and associations with rainfall. J Clim 20:1910–1922

Misra V (2008a) Coupled interactions of the monsoons. Geophys Res Let L12705. doi:10.1029/2008GL033562

Misra V (2008b) Coupled air, sea, and land interactions of the South American monsoon. J Clim 21:6389–6403

Misra V, DiNapoli S (2012) The observed teleconnection between the equatorial Amazon and the Intra-Americas Seas. Clim Dyn. doi:10.1007/s00382-012-1474-1

Misra V, DiNapoli S (2013) The variability of the Southeast Asian summer monsoon. Int J Climatol. doi:10.1002/joc.3735

Misra V, Dirmeyer PA (2009) Air, sea, and land interactions of the continental US hyrdoclimate. J Hydromet 10:353–373

Misra V, Chan S, Wu R, Chassignet E (2009) Air-sea interaction over the Atlantic warm pool in the NCEP CFS. Geophys Res Lett 36:L15702. doi:10.1029/2009GL038525

Mo K et al (2005) Atmospheric moisture transport over the United States and Mexico as evaluated in the NCEP regional reanalysis. J. Hydromet 6:710–728

Mooers CNK, Maul G (1998) Intra-Americas sea circulation. The Sea. In: Robinson A, Brink KH (eds) The global coastal ocean, regional studies and syntheses, vol 11. Wiley, New York, pp 183–208

Moorthi S, Suarez MJ (1992) Relaxed Arakawa-Schubert. A parameterization of moist convection for general circulation models. Mon Weather Rev 120:978–1002

Oey L-Y, Ezer T, Lee H-C (2005) Loop current, rings and related circulation in the Gulf of Mexico: an review of numerical models and future challenges. In: Sturges W, Lugo-Fernandez A (eds) Circulation in the Gulf of Mexico: observation and models. American Geophysical Union, Washington, DC, pp 31–56

Orlanski I, Sheldon J (1995) Stages in the energetics of baroclinic systems. Tellus 47A:605–628

Palmer TN, Doblas-Reyes FJ, Weisheimer A, Rodwell MJ (2008) Toward seamless prediction: calibration of climate change projections using seasonal forecasts. Bull Am Meteorol Soc 89:459–470

Rasmusson EM (1967) Atmospheric water vapor transport and the water balance of North America: part I. Characteristics of the water vapor flux field. Mon Weather Rev 95:403–426

Reynolds RW, Smith TM, Liu C, Chelton DB, Casey KS, Schlax MG (2007) Daily high-resolution blended analyses for sea surface temperature. J Clim 20:5473–5496

Risien CM, Chelton DB (2008) A global climatology of surface wind and wind stress fields from eight years of QuickSCAT scatterometer data. J Phys Oceanogr 38:2379–2413

Ropelewski CF, Halpert MS (1987) Global and regional scale precipitation patterns associated with the El Niño/Southern Oscillation. Mon Weather Rev 115:1606–1626

Rossow WB, Walker AW, Beuschel DE, Roiter MD (1996) International Satellite Cloud Climatology Project (ISCCP) Documentation of new cloud datasets. WMO/TD-No. 737, World Meteorological Organization, 115 pp

Ruiz-Barradas A, Nigam S (2005) Warm season rainfall variability over the U.S. great plains in observations, NCEP and ERA-40 reanalyses, and NCAR and NASA atmospheric model simulations. J Clim 18:1808–1830

Saha S et al (2010) The NCEP climate forecast system reanalysis. Bull Am Meteorol Soc 91:1015–1057

Shchepetkin AF, McWilliams JC (2005) The regional ocean modeling system: a split-explicit, free-surface, topography following coordinates ocean model. Ocean Model 9:347–404

Shukla J, Palmer TN, Hagedorn R, Hoskins B, Kinter J, Marotzke J, Miller M, Slingo J (2010) Towards a new generation of world climate research and computing facilities. Bull Am Meteorol Soc 91:1407–1412

Slingo JM (1987) The development and verification of a cloud prediction model for the ECWMF model. Quart J Roy Meteorol Soc 113:899–927

Song YT, Haidvogel DB (1994) A semi-implicit ocean circulation model using a generalized topography following coordinate system. J Comput Phys 115:228–248

Sturges W, Lugo-Fernandez A (eds) (2005) Circulation in the Gulf of Mexico: observations and models. Geophys Mongr Ser 161:347, AGU, Washington DC. doi:10.1029/GM161

Tiedtke M (1983) The sensitivity of the time-mean large-scale flow to cumulus convection in the ECMWF model. In: Proceedings of ECMWF workshop on convective in large-scale models, Reading, United Kingdom, European Centre for Medium-Range Weather Forecasts, pp 297–316

Wang B, Ding Q, Fu X, Kang IS, Jin K, Shukla J, Doblas-Reyes F (2005) Fundamental challenge in simulation and prediction of summer monsoon rainfall. Geophys Res Lett 32:L15711. doi:10.1029/2005GL022734

Wang C, Enfield DB, Lee SK, Landsea CW (2006) Influences of the Atlantic warm pool on Western Hemisphere summer rainfall and Atlantic hurricanes. J Clim 19:3011–3028

Wu R, Kirtman BP, Pegion K (2006) Local air–sea relationship in observations and model simulations. J Clim 19:4914–4932

Xie P, Arkin PA (1997) Global precipitation: a 17-year monthly analysis based on gauge observations, satellite estimates, and numerical model outputs. Bull Am Meteorol Soc 78:2539–2558

Xue Y, Huang B, Hu Z, Kumar A, Wen C, Behringer D, Nadiga S (2011) An assessment of oceanic variability in the NCEP climate forecast system reanalysis. Clim Dyn 37:2511–2539